arXiv:0712.2604v1 [cond-mat.supr-con] 17 Dec 2007

Thermal conductivity evidence for $d_{x^2-y^2}$ pairing symmetry in the heavy-fermion CeIrIn$_5$ superconductor

Y. Kasahara[1], T. Iwasawa[1], Y. Shimizu[1], H. Shishido[1], T. Shibauchi[1], I. Vekhter[2], and Y. Matsuda[1,3]
[1] *Department of Physics, Kyoto University, Kyoto 606-8502, Japan*
[2] *Department of Physics and Astronomy, Louisiana State University, Baton Rouge, Louisiana, 70803, USA and*
[3] *Institute for Solid State Physics, University of Tokyo, Kashiwanoha, Kashiwa, Chiba 277-8581, Japan*

Quasi-two dimensional CeIrIn$_5$ contains two distinct domes with different heavy fermion superconducting states in its phase diagram. Here we pinned down the superconducting gap structure of CeIrIn$_5$ in the second dome, located away from the antiferromagnetic (AF) quantum critical point, by the thermal transport measurements in magnetic fields $\boldsymbol{H}$ rotated relative to the crystal axes. Clear fourfold oscillation was observed when $\boldsymbol{H}$ is rotated within the ab-plane, while no oscillation was observed within the bc-plane. In sharp contrast to previous reports, our results are most consistent with $d_{x^2-y^2}$ symmetry, implying that two superconducting phases have the same gap symmetry which appears to be mediated by AF spin fluctuations.

PACS numbers: 74.20.Rp,74.25.Dw,74.25.Fy,74.70.Tx

Superconductivity in heavy-Fermion (HF) compounds continues to be a central focus of investigations into strongly correlated electron systems. The relationship between the magnetism and unconventional superconductivity, whereby the gap function $\Delta(\boldsymbol{k})$ has nodes on the Fermi surface where $\Delta(\boldsymbol{k})$=0, is a particularly important theme of research [1]. Many analyses have focused on the scenario of superconductivity (SC) mediated by low energy magnetic fluctuations, often in proximity to a quantum critical point (QCP), where magnetic ordering temperature is driven to zero by an external parameter such as pressure or chemical substitution. Indeed, unconventional SC appears in the vicinity of an antiferromagnetic (AF) QCP in most Ce-based HF compounds, including CeIn$_3$, CePd$_2$Si$_2$ [2], CeCoIn$_5$ [3] and CeRhIn$_5$ [4], as well as organic and high-T_c superconductors.

Notable counter examples have been recently reported in two Ce compounds, in which two distinct domes of different HF superconducting phases appear as a function of pressure or chemical substitution. The first example is the prototypical CeCu$_2$Si$_2$, with one SC dome at low pressure around the AF QCP, and another dome emerging at high pressure distant from the QCP [5]. The superconductivity in the low pressure dome is consistent with the magnetically mediated pairing. On the other hand, Cooper paring resulting from the Ce-valence fluctuations was proposed for the high pressure region, where no discernible AF fluctuations are found [5, 6].

The second example is a quasi-two dimensional (2D) CeIrIn$_5$(T_c=0.4 K) [3], whose phase diagram is shown in the inset of Fig. 1 [7, 8]. In this system the Rh substitution for Ir increases the c/a ratio, acting as a negative chemical pressure that increases AF correlations. In CeRh$_{1-x}$Ir$_x$In$_5$, the ground state continuously evolves from AF metal (AFM) ($x < 0.5$) to superconductivity ($x > 0.5$). T_c shows a maximum at $x \sim 0.7$ and exhibits a cusp-like minimum at x ∼0.9, forming a first dome (SC1). The strong AF fluctuations associated with the AF QCP nearby are observed in SC1 [8, 9]. In CeIrIn$_5$ (x=1), T_c increases with pressure and exhibits a maximum (T_c=1 K) at P ∼3 GPa, forming a second dome (SC2). The AF fluctuations are strongly suppressed with pressure, in SC2, far from the AF QCP [8, 9, 10]. Moreover, the nature of the AF fluctuations in magnetic fields in CeIrIn$_5$ is very different from that in CeCoIn$_5$ and AF CeRhIn$_5$ [11, 12, 13]. Thus the superconductivity in CeIrIn$_5$ at ambient pressure may be distinct from that in CeCoIn$_5$ and CeRhIn$_5$, although all three compounds share similar quasi-2D band structure [14].

Hence a major outstanding question is the nature of the microscopic pairing interaction responsible for the superconductivity in CeIrIn$_5$. By analogy with CeCu$_2$Si$_2$, CeIrIn$_5$ in SC2 was suggested to be a strong candidate for the Ce-valence fluctuation mediated superconductor [6]. To elucidate the pairing interaction, the identification of the superconducting gap structure is of primary importance. Measurements of nuclear quadrupole resonance relaxation rate [9, 10], thermal conductivity [15, 16] and heat capacity [15] revealed that the superconductivity of CeIrIn$_5$ is unconventional, with line nodes in the gap. Very recently, from the measurements of the anisotropy between the interplane and intraplane thermal conductivity κ, the gap function of CeIrIn$_5$ was suggested to be of hybrid type, $k_z(k_x + ik_y)$, or E_g symmetry [16], similar to UPt$_3$ [17], and in sharp contrast to the $d_{x^2-y^2}$ gap in CeCoIn$_5$ (and most likely in CeRhIn$_5$ under pressure) [18]. However, as pointed out in Ref. [19], the anisotropy of κ alone is not sufficient to establish the hybrid gap, and further experiments aimed at clarifying the shape of the superconducting gap are strongly required.

In this Letter, to shed light on the pairing mechanism of CeIrIn$_5$, we performed the thermal transport measurements in magnetic fields $\boldsymbol{H}$ rotated relative to the crystal axes. We provide strong evidence that the gap symmetry is $d_{x^2-y^2}$ of B_{1g} symmetry. These results put a constraint

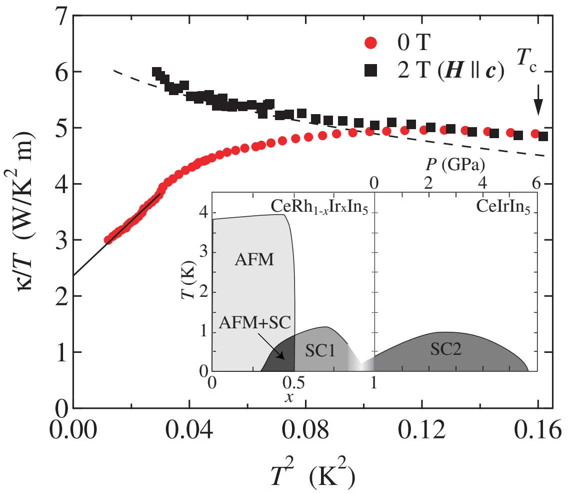

FIG. 1: (Color online) Temperature dependence of κ/T as a function of T^2 in zero field and above H_{c2}^c (H=2 T). Solid line represents $\kappa/T = \kappa_{00}/T + AT^2$; dashed line shows κ/T obtained from the resistivity using Wiedemann-Franz law. Inset: phase diagram of CeIrIn$_5$ as a function of Ir concentration and pressure, from Refs.[7, 8].

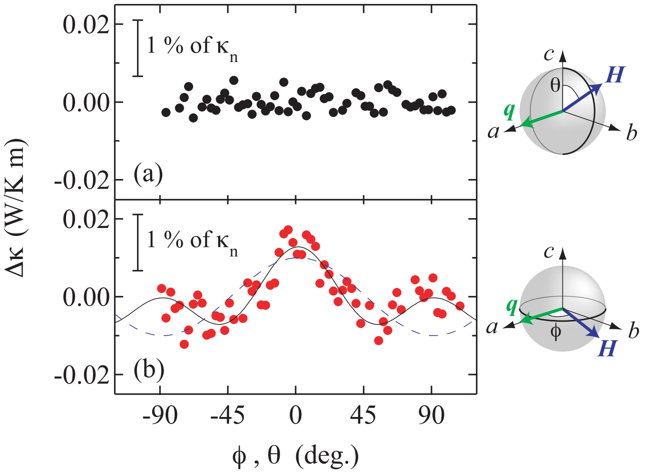

FIG. 2: (Color online) Angular variation of the thermal conductivity, $\Delta\kappa \equiv \kappa - \kappa_0$, at T=200 mK with rotating $\boldsymbol{H}$ (a) within the bc-plane as a function of polar angle θ ($|\boldsymbol{H}|$=0.05 T) and (b) within the 2D ab-plane as a function of azimuthal angle ϕ ($|\boldsymbol{H}|$=0.10 T). Here κ_0 is the angular average of κ. The thermal current $\boldsymbol{q}$ is applied parallel to the a-axis. The dashed line shows the twofold ($\cos 2\phi$) variation. The solid line is the fit by $\kappa(\phi) = \kappa_0 + C_{2\phi}\cos 2\phi + C_{4\phi}\cos 4\phi$, where $\kappa_0, C_{2\phi}$, and $C_{4\phi}$ are constants.

on the pairing mechanism in CeIrIn$_5$.

Single crystals were grown by the self-flux method. The bulk transition temperature is 0.4 K, and upper critical fields parallel to the ab-plane and the c-axis, H_{c2}^{ab} and H_{c2}^{c}, are 1.0 T and 0.5 T at T=0 K, respectively. We measured the thermal conductivity κ along the tetragonal a-axis (heat current $\boldsymbol{q} \| a$) on the sample with a rectangular shape ($2.8 \times 0.45 \times 0.10$ mm^3) by the standard steady state method. To apply $\boldsymbol{H}$ with high accuracy (misalignment of less than 0.05°) relative to the crystal axes, we used a system with two superconducting magnets generating $\boldsymbol{H}$ in two mutually orthogonal directions and dilution refrigerator equipped on a mechanical rotating stage at the top of the Dewar.

Figure 1 depicts the temperature dependence of κ/T as a function of T^2 at $H = 0$ and in the normal state above H_{c2}^c. The overall behavior of κ/T is similar to those reported in Refs. [15] and [16]. In zero field, κ/T decreases with decreasing T after showing a broad maximum at T_c, similar to UPt$_3$ [20] and CePt$_3$Si [21]. The value of κ/T at T_c is nearly 30 % smaller than that reported in Ref. [16] and nearly three times larger than that reported in Ref. [15]. The dashed line is κ/T obtained from the Wiedemann-Franz law, $\kappa/T = L_0/\rho$, where $L_0 = \frac{\pi^2}{3}\left(\frac{k_B}{e}\right)^2$ is the Sommerfeld value and ρ is the measured normal state resistivity. The observed κ/T is close to L_0/ρ, which indicates that the heat transport is dominated by the electronic contribution.

We first discuss the thermal conductivity in zero field. As shown in Fig. 1, κ/T at low T is well fitted by $\kappa/T = \kappa_{00}/T + AT^2$. The presence of a residual term, κ_{00}/T, as $T \to 0$ K is clearly resolved. This term indicates the existence of a residual normal fluid, which is expected for nodal superconductors with impurities. For a gap with line nodes, the magnitude of κ_{00}/T is independent of impurity concentration [22]. The present value of $\kappa_{00}/T \simeq 2.2$ W/K^{2}m is close to that reported in Ref. [16], and, as discussed there, is in good agreement with the theoretical estimate for a superconductor with line node. Thus our thermal conductivity results are also consistent with the presence of line node in the gap function.

The next important question is the nodal topology. Thermal conductivity is a powerful directional probe of the nodal structure: Recent measurements of both κ and the heat capacity with $\boldsymbol{H}$ applied at varying orientation relative to the crystal axes established the superconducting gap structure in $\boldsymbol{k}$-space in several systems [18, 23, 24]. In contrast to fully gapped superconductors, the heat transport in nodal superconductors is dominated by delocalized near-nodal quasiparticles. Applied field creates a circulating supercurrent flow $\boldsymbol{v}_s(\boldsymbol{r})$ associated with vortices. The Doppler shift of the energy of a quasiparticle with momentum $\boldsymbol{p}$, $[E(\boldsymbol{p}) \to E(\boldsymbol{p}) - \boldsymbol{v}_s \cdot \boldsymbol{p}]$, is important near the nodes, where the local energy gap is small, $\Delta(\hat{\boldsymbol{p}}) < |\boldsymbol{v}_s \cdot \boldsymbol{p}|$. Consequently the density of states (DOS) depends sensitively on the angle between $\boldsymbol{H}$ and nodal directions [25]. Clear twofold or fourfold oscillations of thermal conductivity and heat capacity associated with the nodes have been observed in UPd$_2$Al$_3$ [26], YBa$_2$Cu$_3$O$_7$ [27], CeCoIn$_5$ [24, 28] and κ-

(BEDT-TTF)$_2$Cu(NCS)$_2$ [29] when $\boldsymbol{H}$ is rotated relative to the crystal axes.

Figures 2(a) and (b) show the angular variation of the thermal conductivity at 200 mK ($k_BT/\Delta \sim 0.2$) as $\boldsymbol{H}$ is rotated within the bc-plane at $|\boldsymbol{H}|$=0.05 T ($H/H_{c2}^{c}(T)$ $\simeq$0.14) and within the 2D ab-plane at $|\boldsymbol{H}|$=0.1 T ($H/H_{c2}^{ab}(T)$ $\simeq$0.14), respectively. Here $\theta = (\boldsymbol{H},c)$ and $\phi = (\boldsymbol{H},a)$ are the polar and azimuthal angles, respectively. For the field rotated within the ab-plane ($\theta = 90°$) $\kappa(\phi)$ exhibits a distinct oscillation as a function of ϕ, which is characterized by peaks at $\phi = 0°$ and $\pm 90°$ and minima at around $\pm 45°$. As shown by the solid line, $\kappa(\phi)$ can be decomposed into three terms, $\kappa(\phi) = \kappa_0 + \kappa_{2\phi} + \kappa_{4\phi}$, where $\kappa_{2\phi} = C_{2\phi}\cos 2\phi$ and $\kappa_{4\phi} = C_{4\phi}\cos 4\phi$ have the two and four fold symmetry with respect to ϕ, respectively. We note that, as shown by the dashed line, $\kappa(\phi)$ with minima at $\pm 45°$ and peaks at $\pm 90°$ cannot be fitted only by $\kappa_{2\phi}$-term, indicating the presence of the fourfold term. In sharp contrast to $\boldsymbol{H}$ rotating within the ab-plane, no oscillation is observed when rotating $\boldsymbol{H}$ within the bc-plane; the amplitude of the oscillation is less than 0.2% of κ_n if it exists, where κ_n is the normal state thermal conductivity measured above H_{c2}. The $\kappa_{2\phi}$ term arises from the difference between transport parallel and perpendicular to the vortices. Since for $\boldsymbol{H}$ within the bc-plane the field is always normal to $\boldsymbol{q}$, $\kappa_{2\phi}$ term is absent for this geometry.

We address the origin of the fourfold oscillation. Figures 3(a)-(d) display $\kappa_{4\phi}$ normalized by κ_n at 200 mK after the subtraction of κ_0 and $\kappa_{2\phi}$ below $H_{c2}^{ab}(T)$ ($\simeq 0.7$ T). In the normal state above H_{c2}^{ab}, no discernible oscillation was observed (not shown). At 0.69 T just below $H_{c2}^{ab}(T)$, $\kappa_{4\phi}$ exhibits a minimum at $\phi = 0°$ ($C_{4\phi} < 0$). At H=0.5 T, $\kappa_{4\phi}$ oscillation vanishes. Further decrease of H leads to the appearance of distinct $\kappa_{4\phi}$ oscillation that exhibits maximum at $\phi = 0°$ ($C_{4\phi} > 0$) at H=0.1 and 0.25 T. Figure 3(e) shows the H-dependence of $C_{4\phi}/\kappa_n$. There are two possible origins for the fourfold oscillation: (i) the nodal structure and (ii) in-plane anisotropy of the Fermi surface and H_{c2}^{ab}. It should be stressed that the sign of $C_{4\phi}$ just below H_{c2}^{ab} is the same as that expected from the in-plane anisotropy of H_{c2}^{ab} ($H_{c2} \parallel (100) > H_{c2} \parallel (110)$) [30], whereas its sign at low fields is opposite. This immediately indicates that the origin of the fourfold symmetry at low fields is not due to the anisotropy of the Fermi surface or H_{c2}^{ab}. Rough estimate of the amplitude of the fourfold term in layered d-wave superconductors yields $C_{4\phi}/\kappa_n = 0.082\frac{v_F v_F' eH}{3\pi\Gamma\Delta}\ln(\sqrt{32\Delta/\pi\hbar\Gamma})$, where Δ is the superconducting gap, Γ is the QP relaxation rate, v_F and v_F' are the in-plane and out-of-plane Fermi velocities [31]. Using $\Gamma \sim 1.3{\times}10^{11}$ s^{-1}, $2\Delta/k_BT_c \sim 5$, $v_F \sim 1{\times}10^4$ m/s, and $v_F' \sim 5 \times 10^3$ m/s [9, 28] gives $C_{4\phi}/\kappa_n$ ~2%, of the same order as the data. These results lead us to conclude that that the fourfold symmetry at low fields originates from the nodal structure.

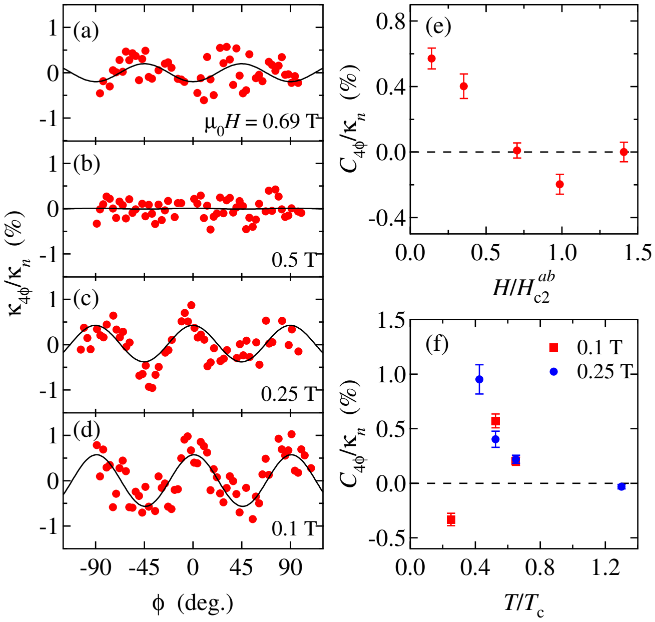

FIG. 3: (Color online) (a)-(d) The fourfold component, $\kappa_{4\phi}$, normalized by κ_n with $\boldsymbol{H}$ rotated in the ab plane at T=200 mK at $|\boldsymbol{H}|$=0.69, 0.5, 0.25, and 0.1 T, respectively. The upper critical field is $H_{c2}^{ab} \gtrsim$0.7 T at this temperature. The solid lines represent the fit by $C_{4\phi}\cos 4\phi$. (e) $C_{4\phi}/\kappa_n$ at T=200 mK as a function of H/H_{c2}^{ab}. (f) $C_{4\phi}/\kappa_n$ at H=0.1 and 0.25 T as a function of T/T_c.

The distinct fourfold oscillation within the ab-plane, together with the absence of the oscillation within the bc-plane, definitely indicates the vertical line nodes perpendicular to the ab-plane, and excludes a horizontal line of nodes at least in the dominant heavy electron bands. Recall that in UPd$_2$Al$_3$ with horizontal line node, clear oscillations of $\kappa(\theta)$ are observed when rotating $\boldsymbol{H}$ within the ac-plane [26]. One could argue that the absence of oscillations within the bc-plane shown in Fig. 2(a) is due to relatively high temperature (k_BT/Δ ~0.2), but the simultaneous observation of the fourfold oscillation within the ab-plane at the same temperature rules out such a possibility.

Thus the superconducting symmetry of CeIrIn$_5$ is narrowed down to either $d_{x^2-y^2}$ or d_{xy}. Further identification relies on the evolution of the oscillations with temperature and field. In the low-T, low-H limit, the Doppler shifted DOS shows a maximum (minimum) when $\boldsymbol{H}$ is along the antinodal (nodal) directions. However, according to recent microscopic calculations, the pattern is inverted at higher T, H due to vortex scattering, and the fourfold components of the specific heat and of the thermal conductivity have similar behavior across the phase diagram [32, 33]. In Fig. 3(f) we plot $C_{4\phi}/\kappa_n$ as a function of temperature. At H=0.1 T, the

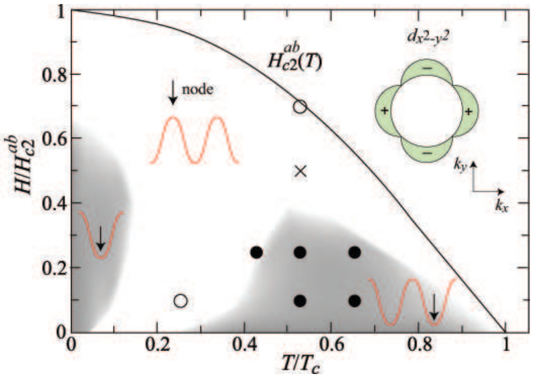

FIG. 4: (Color online) $H-T$ phase diagram for the fourfold term, $\kappa_{4\phi}$, in $\boldsymbol{H}$ rotated within the 2D ab-plane. The solid (open) circles indicate the points where $\kappa_{4\phi}$ shows a maximum (minimum) at $\phi = 0°$. The shaded regions correspond to the region where $\kappa_{4\phi}$ has a minimum at the nodal direction, while $\kappa_{4\phi}$ has a maximum at the nodal directions outside this region [33].

sign change indeed occurs at $T/T_c \simeq 0.25$. Figure 4 displays $H-T$ phase diagram for the fourfold component. The solid (open) circles represent the points at which observed $\kappa_{4\phi}$ exhibits a maximum (minimum) at $\phi = 0°$, and the shading indicates the calculated anisotropy of the thermal conductivity for a d-wave superconductor from Ref. [33]. The shaded (unshaded) regions correspond to the region where $\kappa_{4\phi}$ has a minimum (maximum) for the field in the nodal direction. The calculation was done for a corrugated cylindrical Fermi surface, similar to that of the main FS sheet of CeIrIn$_5$, and the results well reproduce the observed sign change of $\kappa_{4\phi}$. Since the minimum (maximum) of $\kappa_{4\phi}$ occurs at $\phi = 45°$ inside (outside) the shaded region, the nodes are located at ±45°. We thus pin down the gap symmetry of CeIrIn$_5$ as $d_{x^2-y^2}$. While reconciling the existence of vertical lines of nodes with the results of Ref. [16] requires deviations from the perfect cylindrical symmetry of the Fermi surface [19], in the absence of detailed calculations for the realistic band structure of CeIrIn$_5$ (which would be desirable), the agreement with the computed phase diagram is remarkably good.

The $d_{x^2-y^2}$ symmetry implies that the superconductivity is most likely to be mediated by the AF spin fluctuations, not by the Ce-valence fluctuations [34]. Our result is also at odds with the hybrid gap function with horizontal node proposed in Ref. [16]. To our knowledge, CeIrIn$_5$ is the first Ce-based HF compound in which $d_{x^2-y^2}$ symmetry is realized in a distinct superconducting phase remote from the AF QCP. It is intriguing that the superconductivity in SC1 and SC2 phases has the same gap symmetry. A possible explanation for the double dome structure is that the active area on the Fermi surface for the superconductivity, which is nested by magnetic propagation vector $\boldsymbol{Q}=(\frac{1}{2},\frac{1}{2},Q_z)$, has different Q_z in these two phases. In fact, a remarkable difference between CeCoIn$_5$ and CeIrIn$_5$ is that the incommensurate AF order with Q_z=0.298 strongly suppresses the superconductivity in CeRh$_{1-x}$Co$_x$In$_5$ [35], while they coexist in CeRh$_{1-x}$Ir$_x$In$_5$ [36].

In conclusion, the measurements of the thermal conductivity under rotated magnetic fields provide a strong evidence that the superconducting gap of CeIrIn$_5$ at ambient pressure has vertical line nodes, and is of $d_{x^2-y^2}$ symmetry. This indicates that two distinct domes of HF superconducting phases possess the same superconducting symmetry, in which AF fluctuations appear to play an important role. The determined gap symmetry in CeIrIn$_5$ remote from the AF QCP further restricts theories of the pairing mechanism.

We thank H. Ikeda, K. Kontani, P. Thalmeier, and S. Watanabe for helpful discussions.

---

[1] P. Thalmeier and G. Zwicknagl in *Handbook on the Physics and Chemistry of Rare Earths, Vol.34*, (*North Holland* 2005).
[2] N. D. Mathur *et al.*, Nature (London) **394**, 39 (1998).
[3] C. Petrovic *et al.*, J. Phys: Condens. Matter **13**, L337 (2001).
[4] H. Hegger *et al.*, Phys. Rev. Lett. **84**, 4986 (2000).
[5] H. Q. Yuan *et al.*, Science **302**, 2104 (2003).
[6] A. T. Holmes, D. Jaccard, and K. Miyake, J. Phys. Soc. Jpn. **76**, 051002 (2007).
[7] M. Nicklas *et al.*, Phys. Rev. B **70**, 020505(R) (2004).
[8] S. Kawasaki *et al.*, Phys. Rev. Lett. **96**, 147001 (2006).
[9] S. Kawasaki *et al.*, Phys. Rev. Lett. **94**, 037007 (2005).
[10] G.-q. Zheng *et al.*, Phys. Rev. Lett. **86**, 4664 (2001).
[11] J. Paglione *et al.*, Phys. Rev. Lett. **91**, 246405 (2003); A. Bianchi *et al.*, Phys. Rev. Lett. **91**, 257001 (2003); T. Park *et al.*, Nature **440**, 65 (2006).
[12] C. Capan *et al.*, Phys. Rev. B **70**, 180502(R) (2004).
[13] S. Nair *et al.* arXiv:0710.5011.
[14] R. Settai, T. Takeuchi, and Y. Onuki, J. Phys. Soc. Jpn. **76**, 051003 (2007); Y. Haga *et al*, Phys. Rev. B **63**, 060503(R) (2001).
[15] R. Movshovich *et al.* Phys. Rev. Lett. **86**, 5152 (2001).
[16] H. Shakeripour *et al.*, Phys. Rev. Lett. **99**, 187004 (2007).
[17] B. Lussier, B. Ellman, and L. Taillefer, Phys. Rev. Lett. **73**, 3294 (1994).
[18] For review, see Y. Matsuda, K. Izawa, and I. Vekhter, J. Phys.: Condens. Matter **18**, R705 (2006).
[19] I. Vekhter and A. Vorontsov, Phys. Rev. B **75**, 094512 (2007).
[20] H. Suderow *et al.* Phys. Rev. Lett. **80**, 165 (1998).
[21] K. Izawa *et al.* Phys. Rev. Lett. **94**, 197002 (2005).
[22] L. Taillefer *et al.* Phys. Rev. Lett. **79**, 483 (1997).
[23] T. Park and M. B. Salamon, Mod. Phys. Lett. B **18**, 1205 (2004).
[24] T. Sakakibara *et al.*, J. Phys. Soc. Jpn. **76**, 051004 (2007).
[25] I. Vekhter *et al.* Phys. Rev. B **59**, R9023 (1999).
[26] T. Watanabe *et al.*, Phys. Rev. B **70**, 184502 (2004).

[27] H. Aubin *et al.* Phys. Rev. Lett. **78**, 2624 (1997).
[28] K. Izawa *et al.* Phys. Rev. Lett. **87**, 057002 (2001).
[29] K. Izawa *et al.* Phys. Rev. Lett. **88**, 027002 (2002).
[30] F. Weickert *et al.*, Phys. Rev. B **74**, 134511 (2006).
[31] H. Won and K. Maki, cond-mat/0004105
[32] A. Vorontsov and I. Vekhter, Phys. Rev. Lett. **96**, 237001 (2006).
[33] A. Vorontsov and I. Vekhter, Phys. Rev. B **75**, 224501 (2007); Phys. Rev. B **75** 224502 (2007).
[34] For example, K. Tanaka *et al.*, J. Phys.: Condens. Matter **19**, 406219 (2007).
[35] S. Ohira-Kawamura *et al.* Phys. Rev. B, **76**, 132507 (2007).
[36] A. Llobet *et al.* Phys. Rev. Lett. **95**, 217002 (2005).